Electronic Supplementary Material (ESI) for New Journal of Chemistry.
This journal is © The Royal Society of Chemistry and the Centre National de la Recherche Scientifique 2019

Electronic Supplementary Information

Hollow core−shell $NiCo_2S_4$@MoS_2 dodecahedrons with enhanced performance for supercapacitors and hydrogen evolution reaction

Xue-Zhi Song, Fei-Fei Sun, Yu-Lan Meng, Zi-Wei Wang, Qiao-Feng Su and Zhenquan Tan*

State Key Laboratory of Fine Chemicals, School of Petroleum and Chemical Engineering, Dalian University of Technology, 2 Dagong Road, Liaodongwan New District, Panjin 124221, Liaoning, China

Corresponding Author

*E-mail: tanzq@dlut.edu.cn

Fig. S1 XRD patterns of ZIF-67 and NiCo-LDH.

Fig. S2 SEM and TEM image of NiCo-LDH.

Fig. S3 SEM image of $NiCo_2S_4$ counterpart.

Fig. S4 Line-scan elemental profile of a $NiCo_2S_4$@MoS_2 dodecahedron

Fig. S5 N_2 adsorption–desorption isotherms of $NiCo_2S_4$@MoS_2 heterostructures (a) and $NiCo_2S_4$ counterpart (b).

Fig. S6 (a) CV curves at different scan rates, (b) GCD curves at different current densities of the $NiCo_2S_4$ counterpart.

Fig. S7 CV curves of $NiCo_2S_4$@MoS_2 heterostructures and $NiCo_2S_4$ counterpart at 5 mV/s.

Fig. S8 The GCD curves of the first three cycles and last three cycles of $NiCo_2S_4$@MoS_2 heterostructures (a) and $NiCo_2S_4$ counterpart (b).

Fig. S9 CVs in the region of 0.05-0.15 V vs. RHE for $NiCo_2S_4$@MoS_2 heterostructures (a) and $NiCo_2S_4$ counterpart (b).

Fig. S10 Plots showing the extraction of the C_{dl} for $NiCo_2S_4$@MoS_2 heterostructures and $NiCo_2S_4$ counterpart.

Table S1 Comparison of catalytic parameters of different HER catalysts in alkaline

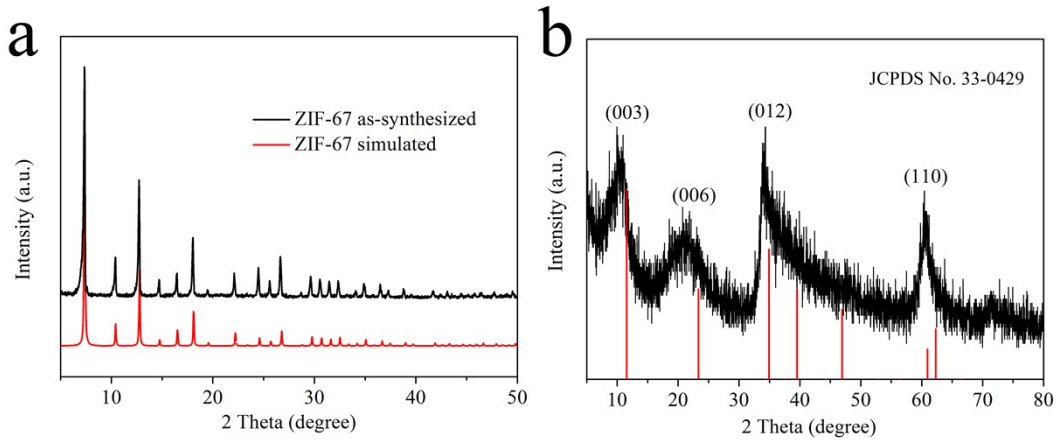

Fig. S1 XRD patterns of ZIF-67 (a) and NiCo-LDH (b).

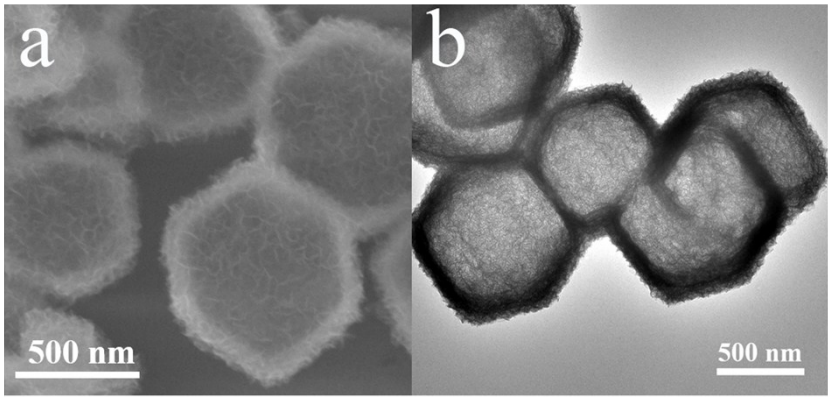

Fig. S2 SEM (a) and TEM image (b) of NiCo-LDH.

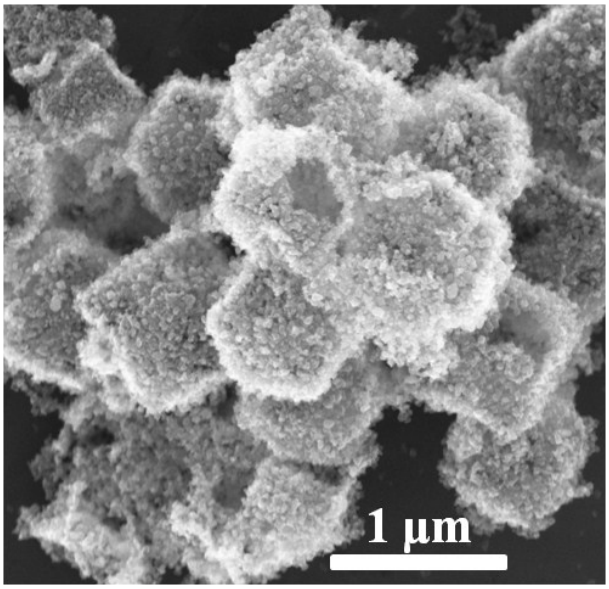

Fig. S3 SEM image of $NiCo_2S_4$ counterpart.

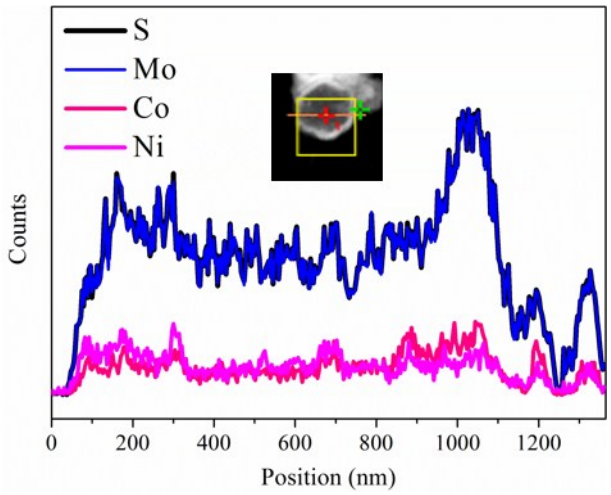

Fig. S4 Line-scan elemental profile of a $NiCo_2S_4$@MoS_2 dodecahedron

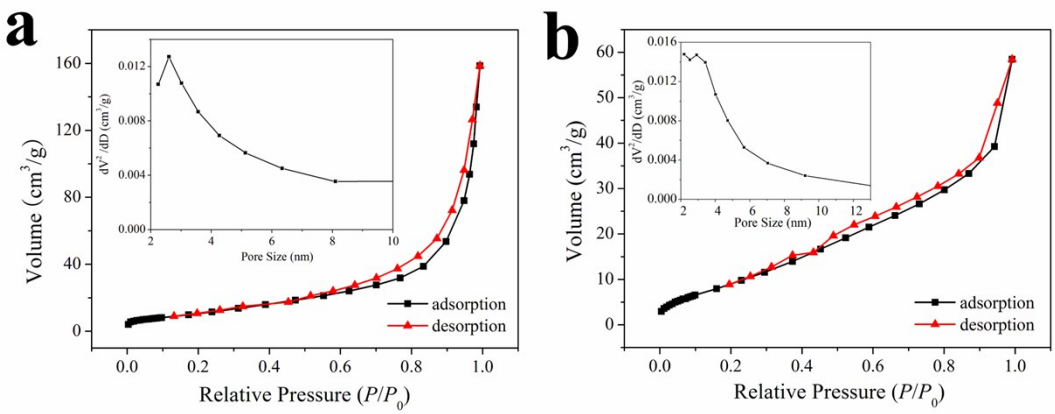

Fig. S5 N_2 adsorption–desorption isotherms of $NiCo_2S_4$@MoS_2 heterostructures (a) and $NiCo_2S_4$ counterpart (b). Insets: The pore diameter distribution

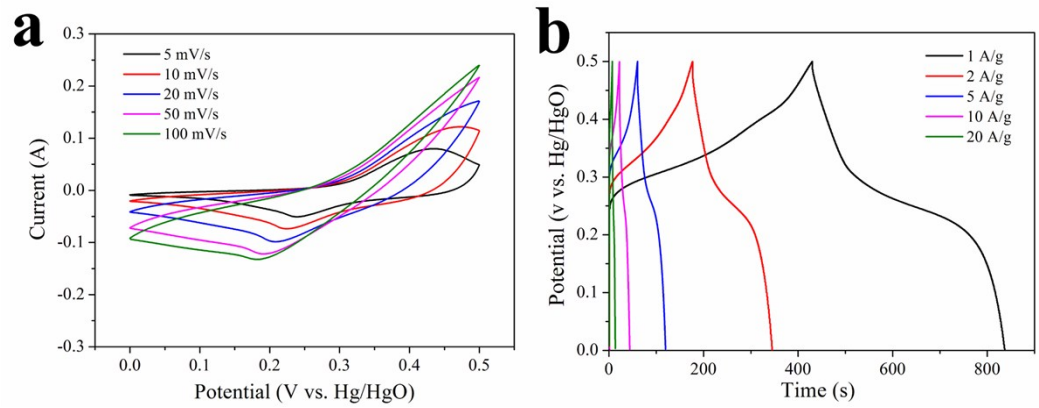

Fig. S6 (a) CV curves at different scan rates, (b) GCD curves at different current densities of the $NiCo_2S_4$ counterpart.

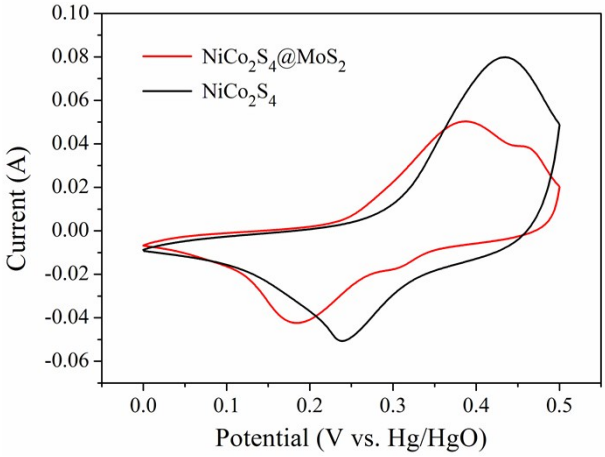

Fig. S7 CV curves of $NiCo_2S_4$@MoS_2 heterostructures and $NiCo_2S_4$ counterpart at 5 mV/s.

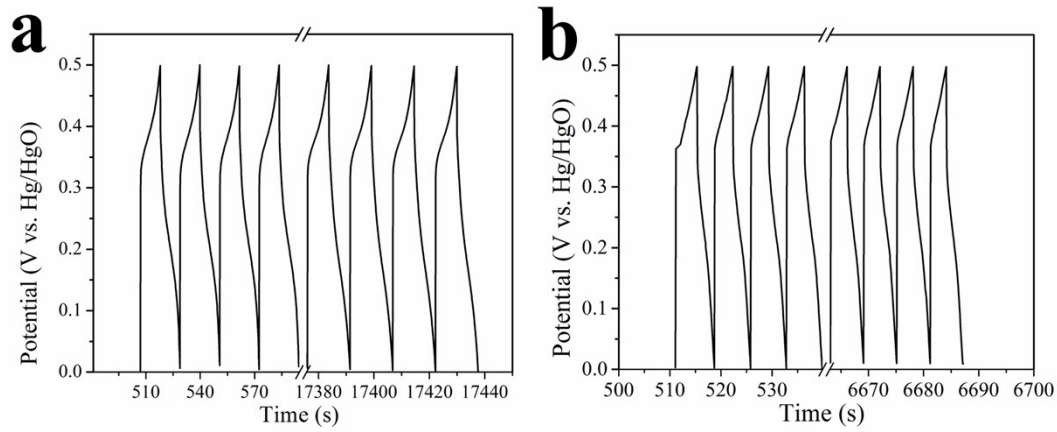

Fig. S8 The GCD curves of the first three cycles and last three cycles of $NiCo_2S_4$@MoS_2 heterostructures (a) and $NiCo_2S_4$ counterpart (b).

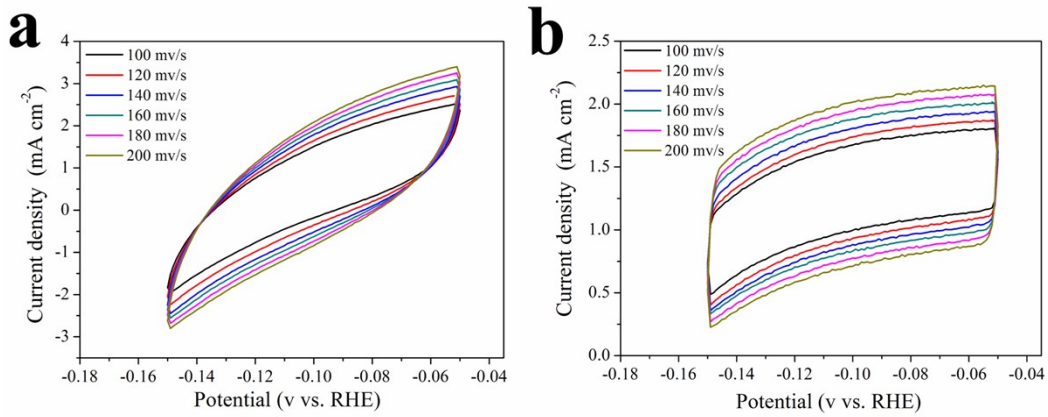

Fig. S9 CVs in the region of 0.05-0.15 V vs. RHE for $NiCo_2S_4$@MoS_2 heterostructures (a) and $NiCo_2S_4$ counterpart (b).

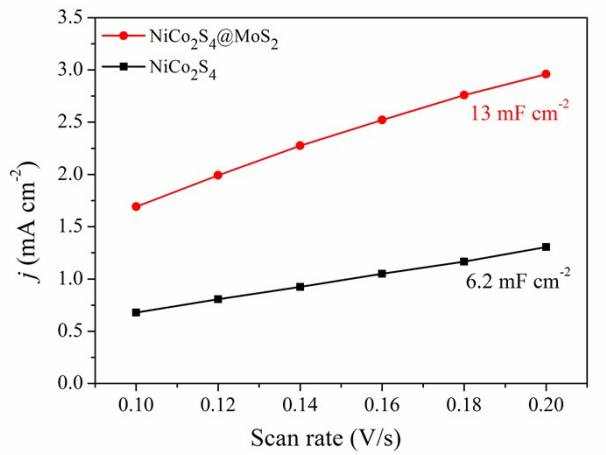

Fig. S10 Plots showing the extraction of the C_{dl} for $NiCo_2S_4$@MoS_2 heterostructures and $NiCo_2S_4$ counterpart.

Table S1 Comparison of catalytic parameters of different HER catalysts in alkaline

Catalyst	Electrolyte	Potential for 10 mA cm^{-2} (V vs. RHE)	Tafel slope (mV dec^{-1})	Ref.
Hollow $NiCo_2S_4$@MoS_2 heterostructures	1 M KOH	-0.194	62	This work
MoS_2/Co_3S_4 hybrid hollow polyhedra	1 M KOH	-0.225	115.3	Electrochim. Acta., 2018, 269, 262-273
one-dimensional and hierarchical CoMoO-S/nickel foam (NF)	1 M KOH	-0.134	87	J. Catal., 2018, 361, 204–213
Co incorporated MoS_2 nanoboxes	1 M NaOH	-0.221	102	Electrochim. Acta , 2018, 276, 81-91
CoS-$Co(OH)_2$@aMoS_{2+x}/NF	1 M KOH	-0.143	68	Adv. Funct. Mater 2016, 26, 7386–7393
NiS-$Ni(OH)_2$@aMoS_{2+x}/NF	1 M KOH	-0.226	81	
Co-MoS_2	1 M KOH	-0.179	62	ACS Nano 2018, 12, 4565-4573